femington

Int. J. Clin. Res. Med. Sci. (2026) 1(2):1–10
Article ID: IJCRMS-2026-078

Pharmacognosy-to-Candidate: Protease-Directed Prioritization of Plant-Derived Glycosides via Minimal Semi-Synthetic Optimization

Richa Singh
richasinghsumi@gmail.com
Independent Researcher

Abstract

This study establishes an integrated pharmaceutical discovery pipeline from medicinal plant profiling to preclinical candidate identification, focusing on SARS-CoV-2 main protease (Mpro) inhibition. Comprehensive LC-ESI-TOF-MS/MS analysis of *Cynanchum acutum* L. identified 46 metabolites, with quercetin-3-O-β-galactoside (Q) characterized as the dominant flavonoid glycoside (3.71 mg/g crude extract) through validated HPTLC/HPLC methods. Strategic semi-synthetic optimization via selective O-alkylation generated two analogues (Q1: 7-benzyl; Q2: 7-bromoethyl) to enhance hydrophobicity and membrane permeability. Antiviral evaluation in Vero-E6 cells demonstrated significant SARS-CoV-2 inhibition, with the crude extract (IC_{50}=23.99 μg/mL, SI=13.66) and benzyl derivative Q1 (IC_{50}=29.21 μg/mL, SI=11.06) showing superior potency over the parent compound Q (IC_{50}=59.73 μg/mL, SI=6.16). Molecular docking revealed preferential Mpro binding for Q1 (-8.34 kcal/mol) through conserved catalytic-site interactions with Cys145 and His41. The workflow exemplifies a minimal-chemistry approach from natural product hit to preclinical candidate, validated through orthogonal analytics and structure-activity relationships.

Keywords

• Medicinal Plants • Molecular Docking • Natural Products • SARS-CoV-2 • Antiviral Agents • Drug Discovery

1. Introduction

The persistent global health challenge posed by SARS-CoV-2 variants necessitates continued development of therapeutic interventions targeting conserved viral mechanisms. Despite World Health Organization declarations regarding pandemic phases, emerging variants maintain significant transmission potential and immune evasion capabilities, underscoring the need for broad-spectrum antiviral strategies [1]. Current FDA-approved therapeutics, including remdesivir, nirmatrelvir/ritonavir, and molnupiravir, face limitations in efficacy against novel variants and accessibility in resource-limited settings [2]. This therapeutic gap motivates exploration of nature-derived scaffolds with established safety profiles and synthetic tractability for lead optimization.

The Apocynaceae family, particularly the *Cynanchum* genus, represents a rich source of structurally diverse secondary metabolites with documented pharmacological activities. Traditional use of *Cynanchum* species in folk medicine as antitussives, analgesics, and anti-inflammatory agents provides ethnobotanical validation for their therapeutic potential [3]. *Cynanchum acutum* L., indigenous to Mediterranean regions and widely distributed in Egypt, has demonstrated antioxidant, anticancer, and antimicrobial properties

in previous investigations [4, 5]. The phytochemical richness of this species, particularly in flavonoid glycosides, positions it as a promising source for antiviral discovery against RNA viruses.

Flavonoid glycosides represent privileged scaffolds in natural product-based drug discovery due to their favorable toxicity profiles, structural diversity, and multifunctional biological activities. Quercetin and its glycosylated derivatives have demonstrated broad-spectrum antiviral activity through various mechanisms, including viral entry inhibition, replication complex disruption, and protease inhibition [6]. However, the inherent hydrophilicity of glycosylated flavonoids often limits cellular permeability and oral bioavailability, necessitating strategic chemical optimization to enhance drug-like properties while preserving bioactive pharmacophores.

The SARS-CoV-2 main protease (Mpro, 3CLpro) represents an attractive therapeutic target due to its essential role in viral replication, high conservation across variants, and absence of closely related human homologs [7]. Mpro functions as a cysteine protease responsible for cleaving viral polyproteins into functional units, making its inhibition a validated strategy for suppressing viral replication [8]. The well-characterized active site architecture, featuring a catalytic dyad of Cys145 and His41 within a substrate-binding cleft, enables structure-based design of small molecule inhibitors.

This study establishes an integrated pharmacognosy-to-candidate pipeline encompassing metabolic profiling, targeted isolation, rational semi-synthesis, biological evaluation, and computational validation. We hypothesize that strategic hydrophobization of quercetin-3-O-β-galactoside through minimal synthetic modification will enhance antiviral potency while maintaining target engagement through conserved interactions with Mpro catalytic residues. The systematic approach demonstrates a reproducible framework for accelerating natural product-based antiviral discovery with translational potential.

2. Materials and Methods

2.1 Plant Material and Extraction

Fully developed specimens of *Cynanchum acutum* L. At Suez Canal University, three different horticultural sites were studied during October 2019. The sites chosen were the Faculty of Pharmacy, Gardens, Commerce Gardens and Nursing Gardens. However, no data pertaining to patients or hospitals were used in this study. All experimental data were prospectively generated from collected plant material and analytical laboratory. Verification of the plant was accomplished by Professor Sayeda Gamal Eldin, Department of Botany, Faculty of Science, Suez Canal University, and a voucher specimen (SAA-157) was deposited at the herbarium of Department of Pharmacognosy. Subjected exhaustively to methanol extraction (4 × 5 L) at ambient temperature with continuous stirring There concentrated extracts were initially concentrated by a rotary evaporator at reduced pressure. 10 kg shade dried powdered mechanically was dried plant material. An examination of methanolic salts was carried on a crude 531 g extract.

The total period of the study for the sample processing, extraction, phytochemical analysis, semi-synthesis and biological evaluation was October 2019 to December 2020. The extraction method followed standard methods with amendments for the enhancement of flavonoid recovery [9]. After conducting a preliminary phytochemical screening, we were able to isolate the solvent that can effectively extract polar flavonoids. Methanol was superior to ethanol and aqueous. The extract in powdered form was stored in crystalline amber glass containers at -20 °C to prevent degradation of labile constituents until analysis.

2.2 LC-ESI-TOF-MS/MS Analysis

The metabolic profiling of the sample was carried out using an LC-ESI-TOF-MS/MS system equipped with an analytical column that has the following characteristics: XSelect HSS T3 analytical column (2.5 μm, 2.1 × 150 mm; Waters). The chromatographic separation utilizing different mobile phases for gradient separation. The mobile phase 'A' consisted of 5 mM ammonium formate (pH 3 and 1% methanol for positive mode), (pH 8 and 1% methanol for negative mode), phase 'B' was 100% acetonitrile. The gradient schedule of the run in reverse-phase HPLC was 0-1 minute (90% A), 1-21 minute (90%→10% A), 21-25 minute (10% A), 25.01-28 minute (90% A) at a flow rate of 0.3 mL/min and column temperature of 40°C.

To prepare the sample, 50 mg of the crude extract was dissolved in 1 mL of mobile phase working solution (water:methanol:acetonitrile, 50:25:25 v/v) through vortex mixing (2 min) and ultrasonication (10 min). Further purification of the samples involved centrifugation (10,000 rpm, 10 min). The supernatant was diluted to 1μg/μL and both ionization modes injected (10μ). Data acquisition used full-scan mode (m/z 50-1,500) and automatic fragmentation (MS/MS) of the ten most intense ions per cycle.

Data Processing was done with MS-DIAL version 3.52 software and MasterView software. The effective signal-to-noise ratio was taken to be > 5% and the sample-to-blank intensity ratio > 5%. The identification was accomplished through accurate mass measurement (mass error < 10% ppm), MS/MS fragmentation pattern, retention time alignment, and database matching. This matching was against ReSpect (negative: n = 1573 records; positive: n = 2737 records) and in-house.

2.3 Isolation and Purification of Quercetin-3-O-β-galactoside

The principal flavonoid constituent, quercetin-3-O-β-galactoside (Q), was isolated as per the conditions of [9] with slight modifications. For the sake of consistency, the compound is named Q hereafter in the rest of the paper. To put it briefly, 531 grams of the crude methanolic extract was suspended in 1.5 liters of distilled water and then sequentially partitioned with n-hexane, chloroform, ethyl acetate, and n-butanol (4 liters each). The ethyl acetate portion (62 g) was subjected to vacuum liquid chromatography using stepwise gradients of n-hexane-ethyl acetate (100:0→0:100) followed by ethyl acetate-methanol (100:0→0:100).

The 35% methanol fractions of eluted ethyl acetate (1.5 g) were purified by column chromatography over silica gel with chloroform-methanol gradients 100:0→0:100 and subsequently with methanol-water gradients 100:0→90:10. Analytical TLC (silica gel 60 F254; ethyl acetate:formic acid:acetic acid:water, 100:11:11:26 v/v/v/v) monitoring of obtained fractions identified those containing Q that were combined and evaporated to yield 630 mg (0.12% w/w from crude extract).

Reverse-phase HPLC with Nucleodur C18 column (125 × 4 mm, 5 μm) was used for purity assessment (Young Line YL9100 system). Isocratic elution (acetonitrile:water, 14:86 v/v) at 0.2 mL/min, detection at 255 nm. Q was detected with a single peak at 3.507 min demonstrating chromatographic purity > 98%.

2.4 HPTLC Quantification

HPTLC analysis was performed according to ICH guidelines [10] using a CAMAG system (Linomat V applicator, TLC Scanner III, winCATS software). Standard solutions of Q (2 μg/μL in methanol) and sample solutions (50 mg/mL crude extract in methanol) were applied (6 mm bands, 10.5 mm track distance) to silica gel 60 F254 plates (20 × 10 cm). Chromatographic development employed ethyl acetate:formic acid:acetic acid:water (100:11:11:26 v/v/v/v) in a twin-trough chamber after 20 min

saturation. Post-development, plates were air-dried and scanned at 350 nm in absorption mode.

Method validation included linearity (100-1100 ng/band), precision (intra-day and inter-day RSD < 2%), accuracy (recovery 97.71%), LOD (22 ng), and LOQ (70 ng). Quantification of Q in crude extract utilized the regression equation (y = 14.955x + 2342) derived from the calibration curve.

2.5 Semi-Synthetic Derivatization

Two semi-synthetic analogs were prepared through selective O-alkylation at the 7-position of Q. All reactions employed dry DMF (molecular sieves, 4Å) under nitrogen atmosphere with progress monitored by TLC (silica gel 60 F254, UV detection).

To a solution of Q (0.22 mmol) of the 7-benzyl derivative in dry DMF (3 mL) at 0°C, K2CO3 (0.24 mmol) and benzyl bromide (0.24 mmol) were added. Ethyl acetate was used to extract the reaction mixture that was stirred at reflux for 12 h. The organic layer underwent drying using MgSO4. Afterwards, it was concentrated and purified using flash chromatography (n-hexane:ethyl acetate, 80:20→40:60). Finally, Q1 was collected as an orange oil with a yield of 85%.

In dry DMF at 0° C, Q (0.22 mmol) was treated with NaH (0.24 mmol) and 1-bromo-2-chloroethane (0.24 mmol) for Q2 (7-bromoethyl derivative). The reaction was run overnight at ambient temperature and was worked up and purified in a similar manner to give the pale oil Q2 (83% yield).

Structural characterization employed ^{1}H-NMR and ^{13}C-NMR spectroscopy (Bruker Ascend Aeon 400 MHz, DMSO-d6). Q1: ^{1}H-NMR δ 7.33-7.63 (m, 7H, aromatic), 5.26 (d, J=6.60 Hz, 2H, CH2). Q2: ^{1}H-NMR δ 4.31 (m, 2H, CH2Br), 3.98 (m, 2H, OCH2).

2.6 Antiviral Activity Assessment

To study antiviral activity, Vero-E6 cells were grown in DMEM with 10% FBS and antibiotics at 37°C with 5% CO_2. SARS-CoV-2 (hCoV-19/Egypt/NRC-3/2020) infected Vero-E6 cells at multiplicity of infection drop 0.1.

Inclusion criteria for test compounds: chromatographic purity ≥ 98% by HPLC, structural confirmation by NMR, and sufficient solubility in DMEM (≥ 100 μg/mL). Exclusion criteria: compounds showing precipitation in cell culture medium, or those with cytotoxicity causing > 30% cell death at the highest concentration tested in the MTT assay prior to antiviral evaluation.

Cytotoxicity was assessed by the MTT assay [11]. Cells were seeded in 96-well plates and treated with test compounds for 24 h. MTT reagent was then added and incubated.

No pure compound was excluded during antiviral screening. All isolated and semi-synthetic compounds meeting purity and solubility inclusion criteria were tested. No additional exclusion of samples or replicates occurred after the initial screening phase.

2.7 Molecular Docking Studies

Molecular docking was performed using AutoDock Vina v1.2.0 [12]. The SARS-CoV-2 Mpro structure (PDB: 8B56) was prepared by removing co-crystallized ligands, water molecules, and ions, then adding polar hydrogens and Kollman charges. The catalytic site was defined around the co-crystallized inhibitor with a grid box (20×20×20 Å) centered on the binding pocket.

Ligand structures were generated, energy-minimized (AMBER forcefield), and converted to PDBQT format using OpenBabel v2.3.1. Docking parameters included exhaustiveness=100, max energy difference=3 kcal/mol, and Lamarckian genetic algorithm. Validation involved re-docking the co-crystallized

Table 1: Metabolites in C acutum Methanolic Extract LC-ESI-TOF-MS/MS

Compound	**RT (min)**	**m/z**	**Formula**	**Note**
Succinic acid	1.12	117.0	$C_4H_6O_4$	Known
Malic acid	1.16	133.0	$C_4H_6O_5$	First report
Catechin	1.26	289.1	$C_{15}H_{14}O_6$	Reported
Quercetin	6.19	303.0	$C_{15}H_{10}O_7$	Reported
Rutin	5.54	609.1	$C_{27}H_{30}O_{16}$	Reported
Quercetin-3-O-G	6.79	465.1	$C_{21}H_{20}O_{12}$	Major constituent
Kaempferol	7.28	287.1	$C_{15}H_{10}O_6$	Reported
Naringenin	9.76	271.1	$C_{15}H_{12}O_5$	Reported

ligand (RMSD=1.10 Å). Binding interactions were analyzed using PyMOL and Discovery Studio Visualizer.

3. Results and Discussion

3.1 Metabolic Profiling of C. acutum Extract

Comprehensive LC-ESI-TOF-MS/MS analysis identified 46 metabolites in the methanolic extract of *C. acutum*, representing diverse chemical classes including organic acids, phenolic compounds, and flavonoids (Table 1). Negative and positive ionization modes enabled detection of both acidic and basic metabolites, with mass accuracy < 10% ppm supporting confident identification.

Flavonoids constituted the predominant class, with 20 identified compounds including both aglycones (diosmetin, fisetin, kaempferide, kaempferol, naringenin, quercetin) and glycosides (quercetin, luteolin, and kaempferol derivatives). The abundance of flavonoid glycosides aligns with previous phytochemical reports on *Cynanchum* species and supports the traditional use of these plants in inflammatory conditions [13].

Remarkably, eleven flavonoids were first recognized in C. acutum, which has expanded the knowledge of phytochemistry of C. acutum. These are datiscin, diosmetin, fisetin, isorhamnetin-3-glucoside, kaempferide, kaempferol-3,7-diglucoside, kaempferol-3-O-rutinoside, luteolin-7-O-neohesperidoside, naringenin, quercetin-3,4'-O-di-beta-glucopyranoside and quercetrin. This flavonoid scaffold has been identified on multiple quercetin glycosides and suggests *C. acutum* chemotaxonomy.

The metabolic profile provides a chemical basis for the observed biological activities of *C. acutum* extracts. The combination of phenolic acids, flavonoid aglycones, and glycosylated flavonoids creates a complex mixture with potential synergistic effects, particularly for antiviral activity where multiple mechanisms may be operative simultaneously.

3.2 Isolation and Quantification of Major Flavonoid

Quercetin-3-O-β-galactoside (Q) was isolated as a major constituent through bioactivity-guided fractionation, with structural confirmation by NMR spectroscopy and comparison with literature data [9]. The isolation yield (630 mg, 0.12% w/w from crude extract) indicates Q represents a significant component of the flavonoid fraction.

HPTLC quantification established a linear response (R^2=0.989) over 100-1100 ng/band, with satisfactory precision (RSD=1.36%), accuracy (recovery=97.71%), and sensitivity (LOD=22 ng, LOQ=70 ng). The concentration of Q in crude extract was determined as 3.71 mg/g, confirming its status as a

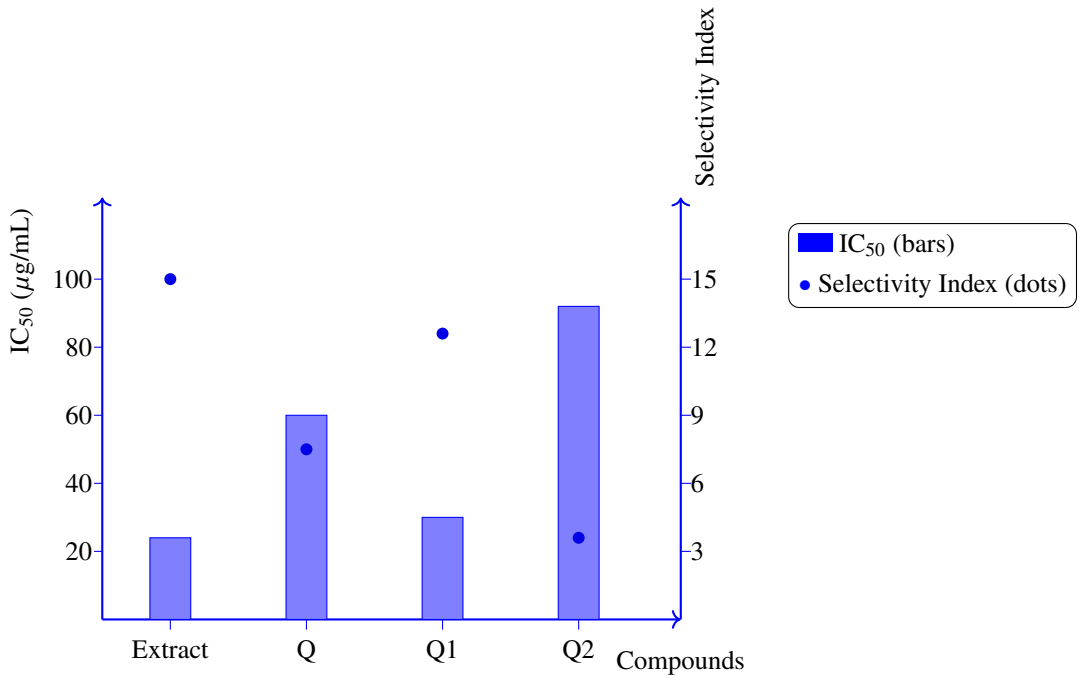

Figure 1: Antiviral activity of *C. acutum* crude extract and isolated compounds (Q, Q1, Q2) against SARS-CoV-2 in Vero-E6 cells. Bars represent IC_{50} values (μg/mL; lower indicates higher potency). Dots represent selectivity index (CC_{50}/IC_{50}; higher indicates improved safety profile). All experiments were performed in triplicate (n=3 independent replicates). Data are presented as mean ± SD. Compound Q1 exhibits the most suitable balance between efficacy and safety.

major flavonoid constituent. The validated HPTLC method provides a rapid quality control tool for standardizing *C. acutum* extracts based on Q content.

HPLC analysis confirmed the chromatographic purity of isolated Q (< 98%), with a single peak at 3.507 min under isocratic conditions. The purity assessment is critical for ensuring that biological activities attributed to Q are not confounded by minor impurities. The combination of HPTLC and HPLC provides orthogonal validation of both identity and purity, establishing a robust analytical foundation for subsequent semi-synthetic and biological studies.

The isolation of Q as a major component aligns with previous reports on *C. acutum* phytochemistry [14] and supports its selection as a scaffold for semi-synthetic optimization. As a glycosylated flavonoid, Q possesses the characteristic chromone scaffold with 3',4'-dihydroxyphenyl substitution at C-2, galactosyl moiety at C-3, and hydroxyl groups at C-5 and C-7, providing multiple sites for chemical modification.

3.3 Semi-Synthetic Optimization Strategy

Strategic semi-synthetic modification targeted the 7-hydroxyl group of Q for alkylation, based on its superior steric accessibility and resonance stabilization compared to other phenolic hydroxyls. This regioselective approach aimed to enhance hydrophobicity while preserving key pharmacophoric elements, particularly the catechol moiety (3',4'-dihydroxyphenyl) implicated in antioxidant and metal-chelating activities.

The synthetic routes employed straightforward nucleophilic substitution reactions under basic conditions, yielding two analogs with distinct hydrophobic character: Q1 (7-benzyl) and Q2 (7-bromoethyl). The benzyl group in Q1 provides substantial hydrophobicity and potential for π-π

stacking interactions, while the bromoethyl moiety in Q2 introduces both hydrophobicity and potential for further functionalization.

Structural characterization by ^{1}H-NMR confirmed successful derivatization through appearance of new signals corresponding to the introduced substituents. For Q1, aromatic protons (7.33-7.63 ppm) and benzyl methylene protons (5.26 ppm) evidenced benzylation. For Q2, ethylenic protons (4.31 ppm, 3.98 ppm) confirmed bromoethyl incorporation. The preservation of sugar moiety signals indicated selective modification at the 7-position without glycosidic cleavage.

Computational analysis using SwissADME predicted improved physicochemical properties for the derivatives. The parent compound Q exhibits high polarity (Log S=-3.04, solubility=0.423 mg/mL), which may limit membrane permeability. Introduction of hydrophobic groups in Q1 and Q2 was anticipated to enhance cellular uptake while maintaining sufficient aqueous solubility for biological testing.

The minimal synthetic approach demonstrates an efficient strategy for natural product optimization, requiring only one-step transformations from the isolated scaffold. This contrasts with more extensive synthetic campaigns that may compromise natural product integrity or require complex protection/deprotection sequences. The semi-synthetic derivatives maintain the core flavonoid structure while modulating physicochemical properties relevant to drug disposition.

3.4 Antiviral Activity and Cytotoxicity Profiling

Comprehensive antiviral evaluation against SARS-CoV-2 in Vero-E6 cells revealed significant differences in potency among the tested compounds (Table 2). The crude methanolic extract demonstrated the highest antiviral activity (IC50=23.99 μg/mL) with favorable selectivity (SI=13.66), suggesting potential synergistic interactions among multiple constituents.

Table 2: Antiviral Activity and Cytotoxicity of Tested Compounds Against SARS-CoV-2 in Vero-E6 Cells

Test compound	**IC_{50} (μg/mL)**	**CC_{50} (μg/mL)**	**Selectivity index (CC_{50}/IC_{50})**
Crude methanolic extract	23.99 ± 1.83	327.9 ± 12.4	13.66
Quercetin-3-O-galactoside (Q)	59.73 ± 3.23	368.3 ± 15.1	6.16
Benzyl derivative (Q1)	29.21 ± 2.13	323.3 ± 11.8	11.06
Bromoethyl derivative (Q2)	91.16 ± 4.73	321.3 ± 13.2	3.42

Among the pure compounds, the benzyl derivative Q1 exhibited superior antiviral potency (IC50=29.21 μg/mL, SI=11.06) compared to the parent Q (IC50=59.73 μg/mL, SI=6.16). This 2-fold enhancement in activity, coupled with maintained cytotoxicity profile, validates the semi-synthetic optimization strategy. The improved activity of Q1 may result from enhanced cellular permeability due to increased hydrophobicity, facilitating intracellular accumulation and target engagement.

In contrast, the bromoethyl derivative Q2 showed reduced antiviral activity (IC50=91.16 μg/mL, SI=3.42), indicating that not all hydrophobic modifications confer beneficial effects. The decreased potency may reflect suboptimal steric or electronic properties for target interaction, or potential reactivity of the bromoethyl moiety leading to non-specific binding or reduced stability.

The cytotoxicity profiles were generally favorable, with CC50 values exceeding 300 μg/mL for all compounds. The similar cytotoxicity across compounds suggests that the introduced modifications did not introduce significant off-target toxic effects at the concentrations tested. The selectivity indices (all compounds showed SI > 3) indicate a reasonable therapeutic window for antiviral effects.

The superior activity of the crude extract compared to isolated compounds suggests potential synergism among multiple constituents. Previous reports have documented enhanced bioactivity of whole plant

extracts compared to isolated components, possibly due to multi-target effects or improved bioavailability of active constituents in complex mixtures [15]. The presence of multiple flavonoid glycosides in the extract may provide complementary mechanisms against viral replication.

3.5 Molecular Docking Analysis

Molecular docking studies provided insights into the potential mechanism of antiviral activity through SARS-CoV-2 Mpro inhibition. Validation of the docking protocol through re-docking the co-crystallized ligand yielded satisfactory RMSD (1.10 Å), supporting the reliability of predicted binding modes.

All tested compounds demonstrated favorable binding energies compared to the co-crystallized inhibitor (-7.51 kcal/mol), with Q1 exhibiting the most favorable score (-8.34 kcal/mol), followed by Q (-7.72 kcal/mol) and Q2 (-7.22 kcal/mol). The correlation between docking scores and experimental antiviral activity for Q and Q1 supports Mpro as a relevant target for these compounds.

Analysis of binding interactions revealed distinct patterns among the compounds (Fig. 2). Q1 established multiple favorable contacts with key catalytic residues, including hydrogen bonds with Cys145 (2.2 Å) and Gln189 (1.8 Å), and π-H interactions with His41 (4.1 Å) and Glu166 (4.0 Å). Engagement of the catalytic dyad (Cys145-His41) is particularly significant, as these residues are essential for protease activity [16].

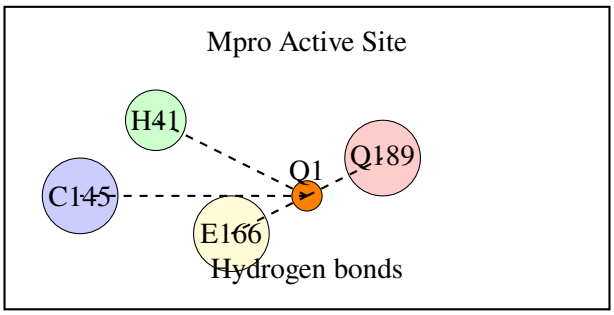

Figure 2: Schematic representation of Q1 binding interactions with key residues in the SARS-CoV-2 Mpro active site (PDB: 8B56). Hydrogen bonds are shown as dashed arrows with distances in Å. π-H interactions are indicated by curved arrows. The catalytic dyad residues (Cys145, His41) are highlighted. Docking was performed using AutoDock Vina with exhaustiveness=100. The figure represents the lowest-energy binding pose from 10 independent docking runs.

The parent compound Q formed hydrogen bonds with His41 (2.1 Å), Asn142 (3.3 Å), and Ser144 (2.6 Å), but lacked direct interaction with Cys145. This difference in binding mode may contribute to the superior activity of Q1 compared to Q. The benzyl group in Q1 appears to facilitate additional hydrophobic contacts within the S2 subsite, potentially enhancing binding affinity.

Q2, despite reasonable docking energy, showed fewer specific interactions with catalytic residues, primarily engaging His41 (2.5 Å) and Asn142 (2.9 Å) through hydrogen bonds. The reduced interaction network may explain its lower experimental activity, despite favorable computational prediction.

The docking results align with structure-activity relationships observed in the antiviral assays, supporting Mpro inhibition as a plausible mechanism contributing to the observed activity. However, the complex viral replication cycle involves multiple potential targets, and additional mechanisms such as RNA-dependent RNA polymerase inhibition or viral entry blockade cannot be excluded based on these data alone.

4. Conclusion and Future Perspectives

This study establishes an integrated pipeline from medicinal plant profiling to preclinical candidate identification, demonstrating the value of natural products as starting points for antiviral discovery. The systematic approach encompassing metabolic characterization, targeted isolation, rational semi-synthesis, biological evaluation, and computational analysis provides a reproducible framework for natural product-based drug discovery.

The strategic semi-synthesis of the benzyl derivative Q1 from the major constituent quercetin-3-O-β-galactoside yielded a promising anti-SARS-CoV-2 candidate with enhanced potency (~2-fold improvement vs. parent compound) and a maintained safety profile, demonstrating the value of minimal synthetic optimization of natural products.

Molecular docking studies support Mpro inhibition as a contributing mechanism, with Q1 establishing favorable interactions with key catalytic residues. The correlation between computational predictions and experimental results validates the structure-based approach for guiding natural product optimization.

Future work should focus on several key areas: First, comprehensive mechanistic studies to confirm Mpro inhibition and identify potential additional targets. Second, evaluation against emerging SARS-CoV-2 variants to assess breadth of activity. Third, pharmacokinetic profiling to establish oral bioavailability and metabolic stability. Fourth, exploration of additional synthetic modifications to further optimize potency and drug-like properties.

The integrated pharmacognosy-chemistry-biology-computation workflow exemplified in this study provides a template for accelerating natural product-based drug discovery against emerging viral threats. By combining traditional knowledge with modern analytical and synthetic approaches, this strategy leverages the structural diversity of natural products while addressing limitations through rational optimization.

References

[1] Melissa M Higdon, Bridget Wall, Chloe B Jones, Joseph G Rosen, Sarah A Tucker, Anna Bałazy, et al. A systematic review of coronavirus disease 2019 vaccine efficacy and effectiveness against severe acute respiratory syndrome coronavirus 2 infection and disease. *Open Forum Infectious Diseases*, 2022.

[2] U.S. Food and Drug Administration. Coronavirus (covid-19) drugs, 2023. URL `https://www.fda.gov/drugs/emergency-preparedness-drugs/coronavirus-covid-19-drugs`.

[3] Hua-Xiang Wang and T B Ng. Natural products with hypoglycemic, hypotensive, hypocholesterolemic, antiatherosclerotic and antithrombotic activities. *Life Sciences*, 65(25):2663–2677, 1999.

[4] G A Fawzy, H M Abdallah, M S A Marzouk, F M Soliman, and A A Sleem. Antidiabetic and antioxidant activities of major flavonoids of cynanchum acutum l.(asclepiadaceae) growing in egypt. *Zeitschrift für Naturforschung C*, 63(9-10):658–662, 2008.

[5] A Youssef, Z El-Swaify, Y Al-aratheh, and S Dalain. Cytotoxic activity of methanol extract of cynanchum acutum l. seeds on human cancer cell lines. *Latin American Journal of Pharmacy*, 37 (10):1997–2003, 2018.

[6] B Dinda, M Dinda, S Dinda, P S Ghosh, and S K Das. Anti-sars-cov-2, antioxidant and immunomodulatory potential of dietary flavonol quercetin: focus on molecular targets and clinical efficacy. *European Journal of Medicinal Chemistry Reports*, 10:100125, 2024.

[7] Hai Yang, Maojun Yang, Yi Ding, Yijin Liu, Zhiyong Lou, Zhaohui Zhou, et al. The crystal structures of severe acute respiratory syndrome virus main protease and its complex with an inhibitor. *Proceedings of the National Academy of Sciences*, 100(23):13190–13195, 2003.

[8] Qing Hu, Ying Xiong, Guo-Hui Zhu, Yi-Ning Zhang, Yi-Wei Zhang, Peng Huang, et al. The sars-cov-2 main protease (mpro): structure, function, and emerging therapies for covid-19. *MedComm*, 3 (3):e151, 2022.

[9] Reda F A Abdelhameed, Ahmed K Ibrahim, Mohamed A Elfiky, Eman S Habib, Mohamed I Mohamed, Eman T Mehanna, et al. Antioxidant and anti-inflammatory activity of cynanchum acutum l. isolated flavonoids using experimentally induced type 2 diabetes mellitus: biological and in silico investigation for nf-kb pathway/mir-146a expression modulation. *Antioxidants*, 10(11): 1713, 2021.

[10] Sylvia K Branch. Guidelines from the international conference on harmonisation (ich). *Journal of Pharmaceutical and Biomedical Analysis*, 38(5):798–805, 2005.

[11] Ahmed Mostafa, Ahmed Kandeli, Yaseen A M M Elshaier, Omnia Kutkat, Yassmin Moatasim, Alaa A Rashad, et al. Fda-approved drugs with potent in vitro antiviral activity against severe acute respiratory syndrome coronavirus 2. *Pharmaceuticals*, 13(12):443, 2020.

[12] Jerome Eberhardt, Diogo Santos-Martins, Andreas F Tillack, and Stefano Forli. Autodock vina 1.2.0: New docking methods, expanded force field, and python bindings. *Journal of Chemical Information and Modeling*, 61(8):3891–3898, 2021.

[13] S Heneldi, R J Grayer, G C Kite, and M S J Simmonds. Flavonoid glycosides from egyptian species of the tribe asclepiadeae (apocynaceae subfamily asclepiadoideae). *Biochemical Systematics and Ecology*, 34(7):575–584, 2006.

[14] I Yildiz, O Sen, R Erenler, I Demirtas, and L Behcet. Bioactivity-guided isolation of flavonoids from cynanchum acutum l. subsp. sibiricum (willd.) rech. f. and investigation of their antiproliferative activity. *Natural Product Research*, 31(22):2629–2633, 2017.

[15] Abeer M El Sayed, Samar M Basam, Eman M B A El-Naggar, M M Marzouk, and Seham S El-Hawary. Lc-ms/ms and gc-ms profiling as well as the antimicrobial effect of leaves of selected yucca species introduced to egypt. *Scientific Reports*, 10(1):17778, 2020.

[16] Daniel W Kneller, Gwyndalyn Phillips, Kevin L Weiss, Shusil Pant, Qiu Zhang, Hugh M O'Neill, et al. Unusual zwitterionic catalytic site of sars-cov-2 main protease revealed by neutron crystallography. *Journal of Biological Chemistry*, 295(50):17365–17373, 2020.